

<https://doi.org/10.1590/2318-0331.272220210110>

Challenges of defining the floodplain through the “mean ordinary flood line” approach using remote sensing in Brazil: a case study of the São Francisco River

Desafios na delimitação de planície de inundação usando o conceito de “linha média de enchentes ordinárias” usando sensoriamento remoto no Brasil: um estudo de caso no Rio São Francisco

Philippe Maillard¹ , Marília Ferreira Gomes² , Évelyn Márcia Pôssa³  & Ramille Soares de Paula⁴ 

¹Universidade Federal de Minas Gerais, Belo Horizonte, MG, Brasil

²Instituto Nacional de Colonização e Reforma Agrária, Belo Horizonte, MG, Brasil

³Instituto de Desenvolvimento Sustentável Mamirauá, Tefé, AM, Brasil

⁴Superintendência do Patrimônio da União de Minas Gerais (SPU-MG), Belo Horizonte, MG, Brasil

E-mails: philippermaillard@yahoo.com.br (PM), mariliafgomes@yahoo.com (MFG), evelynpossa@yahoo.com (EMP), ramille.paula@economia.gov.br (RSP)

Received: September 15, 2021 - Revised: February 07, 2022 - Accepted: February 09, 2022

Abstract

The “Mean Ordinary Flood Line” (MOFL) is a conceptual line adopted by Brazil’s Federal Government to delineate land within the floodplain under its ownership and jurisdiction having major social implications. Past attempts at the cartography of this line have encountered strong difficulties brought either by a low precision or an excessive cost. In this article, we propose a method based on historical water gauge data to determine the water level corresponding to the MOFL. Satellite images coincident with past dates when the MOFL was reached are selected and processed to extract the water surface from which the MOFL can then be produced. The approach was implemented in a 600 km reach of the São Francisco River in Minas Gerais as a pilot project. A field survey served to validate the results. The positional accuracy of the MOFL was estimated at 24 m which was considered excellent since mostly Landsat images with a spatial resolution of 30 m were used.

Keywords: Floodplains; Satellite images; Land management; Water stage; Image classification.

Resumo

A “Linha Média de Enchente Ordinária” (LMEO) é uma linha conceitual adotada pelo Governo Federal do Brasil para delinear terras dentro da planície de inundação sob sua propriedade e jurisdição com importantes implicações sociais. As tentativas passadas de cartografia desta linha encontraram dificuldades de baixa precisão ou de custo excessivo. Neste artigo, propõe-se um método baseado em dados históricos de nível de água para determinar o nível correspondente à LMEO. Imagens de satélite coincidentes com datas anteriores quando o LMEO foi alcançada foram selecionadas e processadas para extrair a superfície da água da qual a LMEO pode então ser produzida. A abordagem foi implementada em um trecho de 600 km do Rio São Francisco, em Minas Gerais, como um projeto piloto. Uma pesquisa de campo serviu para validar os resultados. A precisão posicional do LMEO foi estimada em 24 m, o que foi considerado excelente, pois foram utilizadas principalmente imagens Landsat com resolução espacial de 30 m.

Palavras-chave: Planície de inundação; Imagem de satélite; Manejo do território; Nível de água; Classificação de imagem.

INTRODUCTION

The identification of areas susceptible to flooding is essential for reducing the damage associated with these events and for social harmony and life preservation (Kourgialas & Karatzas, 2011). In many countries, governments and other agencies have invested much efforts in mapping, modelling and monitoring floods to evaluate inundation risks, prevent loss of human life and material damage and to guarantee insurance payments (Monmonier, 1997; Roy et al., 2003; Notti et al., 2018). Flood frequency is intimately linked to the concept of flood returning period by which floods are characterised by the length of time between their recurrence. Usually, a flood with a returning period of a 100 years will have a more dramatic impact than a 10 year flood. This does not, however, give insight on the amount of impact or the destructive power of floods. Even a 100-year returning flood can have little impact to human settlements if the river channel is a canyon or is banked by a large inhabited wetland or forest. Still, mapping the 100-year flood hazard is not enough to map flood risk, since it is also necessary to have an estimate of the local vulnerability or damage associated with a flood. Rather it is the flood susceptibility that can help estimate the amount of risk (vulnerability) an inundation will cause to a specific area (Gallopín, 2006; Kourgialas & Karatzas, 2011). Since damage caused by floods can have major implications for governments (lives, rescue missions, health issues, infrastructure, etc.), it is only natural that policies restrict some activities in marginal lands and floodplains, hence the need to defined these areas is a major stake. In recent years, many authors have published methods for mapping the flood susceptibility of flood-prone areas using geographic information systems (GIS) and advanced processing techniques such as multi criteria analysis (MCA), decision tree (DT), artificial neural network (ANN) and other machine learning approaches (Tehrany et al., 2015; Janizadeh et al., 2019; Bui et al., 2020). Most of these approaches use at least some data derived from remote sensing technologies like digital elevation models (DEM), vegetation indices (VI), wetness indices (WI) and surface water areas extracted from optical or radar image data (Bui et al., 2020). These approaches provide invaluable tools to help decision makers establish policies and regulations to reduce the risks associated with flooding in marginal lands located near rivers. Governments around the world frequently have specific policies regarding marginal lands located in floodplains:

- In the United States of America, the national standard for floodplain management allows encroachments to reduce natural channel size, to divert flood waters and to alter its velocity without much consideration to the effect these changes will cause to other people and property in the watershed (Turner, 2014). Conversely, the National Flood Insurance Program (NFIP) is a federal program that requires local governments instances to regulate construction in floodplain before residents can purchase flood insurance (Holway & Burby, 1990). The “No Adverse Impact” (NAI) principle offers local governments an instrument to regulate construction in floodplains. The NAI states that the action of one property owner cannot adversely affect the rights of other property owners (Turner, 2014). In urban areas, the Federal Emergency Management Agency

(2020), determined that “Floodway surcharge values must be between zero and 1.0 ft. (~30 cm). If the state (or other jurisdiction) has established more stringent regulations, these regulations take precedence over the NFIP regulatory standard” (Federal Emergency Management Agency, 2020). It is understood that “Floodway surcharge” is measured by the water level exceeding the normal high water level;

- The Canadian government created a Flood Damage Reduction Program (FDRP) by which over 320 flood-risk areas covering more than 900 communities were identified. These flood-prone areas were also legally designated. A series of guidelines, the “Federal Flood Mapping Guidelines Series” including “Flood Hazard Maps” and “Flood Awareness Maps” were created to help local governments protect themselves against flood events (Natural Resources Canada, 2018);
- In the United Kingdom, the Flood and Water Management Act 2010 requires Risk Management Authorities (Environment Agency, Lead Local Flood Authorities, District and Borough Councils, Coast protection authorities, Water and sewerage companies, Internal Drainage Boards, Highways authorities) to 1) co-operate with each other; 2) act in a manner that is consistent with the National Flood and Coastal Erosion Risk Management Strategy for England and the local flood risk management strategies developed by Lead Local Flood Authorities; and 3) exchange information (Local Government Association, 2021);
- In Europe, the Common Agricultural Policy (CAP), the Water Framework Directive (WFD), the Birds and Habitat Directives (BHD) (including its resulting Natura 2000 network) recognize the flood protection role of floodplains and has been providing support and financial incentives for pre-defined restrictions on agriculture in floodplains to support the regulating service of the agro-ecological landscape (Wood & van Halsema, 2008).

In Brazil, identifying flood-prone areas also plays an important role in the definition of ownership and dwelling rights (Brasil, 1868, 2012). The Constitution of the Federate Republic of Brazil has been reaffirming its property rights on marginal lands which has been defined in the Brazilian constitution since 1867 (Brasil, 1867, 1988). These rights define as government-owned areas such as “lakes, rivers and any watercourses on land within its domain, or bathing more than one state, serve as borders with or extend to or from foreign territory, as well as marginal land and river beaches”. Marginal lands are those bathed by rivers, lakes or any federal navigable water course and out of reach of tides (Brasil, 2019). It implies that the more than 900 federal rivers, which add up to over 100 000 km of extension, with their marginal land areas of currently unknown size (Figure 1a) are under the responsibility of the Federal Government through its Secretary of Patrimony (Secretaria de Patrimônio da União - SPU). It should be stated that the Brazilian territory is still characterised by a fragility of rights regarding the ownership of rural land and the separation between what is public and private land is still largely undetermined (Guedes & Reydon, 2012). The SPU is therefore responsible for establishing this territory through the

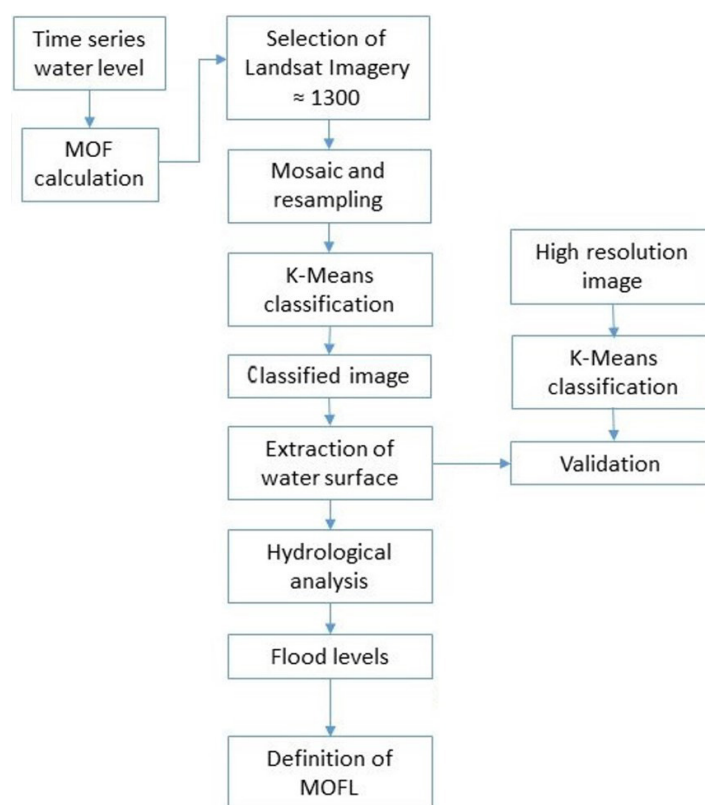


Figure 1. Flowchart of the steps to define the Mean Ordinary Flood Line using satellite image analysis and water gauge data.

concepts of “Mean Ordinary floods” (MOF) and “Mean Ordinary Flood Line” (MOFL, the term “Mean Ordinary Flood Line” is a translation of the portuguese expression *Linha Média de Enchente Ordinária* – LMEO). The justification behind excluding marginal land areas from private domain are multiples: they are subject to frequent flooding, are strategically located, represent sources of tax collection (being government owned), and are an instrument of environmental protection. For the environmental aspect, floodplains hosts the major part of the riparian vegetation which helps maintain the quality of the waters by filtering overland flow, lowering the water temperature and preventing erosion of the river banks (Döringer & Tockner, 2008). For agriculture, the floodplain areas are known to be more fertile than the surrounding drier land and have always been privileged by dwellers for their agricultural potential (Tiner, 2016). Additionally, they have been considered to have the highest ecological value for the ecological services they provide (Costanza et al., 1997). Historically these areas have also been coveted for providing access to communication routes and navigation. Conversely, they are also frequently flooded and the scene of great natural disasters that continue to cause loss of human lives and serious material damage worldwide (Brázdil et al., 2006). For instance, in the United States of America, as a result of developments in floodplains, floods have caused about 200 death and \$9 billions (data from 1990) in property damage yearly (Holway and Burby, 1990). In Germany and Belgium, the month of July 2021 has brought floods caused by the rapid rise of the Rhine and Meuse rivers causing more than a hundred deaths and over a thousand missing. It was characterized the worst deluge recorded in the region in more than 200 years (CBS News, 2021;

BBC News, 2021). The economic impact of floods is a major concern in Brazil. For instance it was determined that the floods of 2008 reduced the São Paulo Gross Regional Product by 0.0263% and the national GRP by 0.0071% (Haddad & Teixeira, 2015). The same year, floods in Santa Catarina (Southern Brazil) caused deadly mudslides resulting in 120 casualties and left 69 000 out of their homes covering an area of over 22000 km² (Ávila et al., 2016). In the State of Rio de Janeiro, the 2008 floods caused 916 deaths and 35000 homeless. The Itajaí River in Santa Catarina is one of the most flood-prone area of Brazil. The water level frequently surpasses the 8-m level and in 2011 it reached 13 m (second highest in the history of the Rio do Sul River, Santa Catarina) with disastrous impacts causing the displacement of 15000 people, making 3000 homeless and producing material damages in excess of R\$283 million (~US\$140 million; Ávila et al., 2016; Bogo, R. S., 2020).

Analyzing the period 1975-2015, Bartiko et al. (2019) determined a positive trend in the frequency and magnitude of floods in the South, North and in parts of South-East Brazil. Conversely they found the opposite is true in almost all the North-East and the remainder of the South-East. This suggest that floods are more frequent and intense in wetter parts of Brazil and less frequent in drier parts.

In Brazil, marginal lands are also used as part of the policies of landholding regularization, recognising the rights of traditional population, formed by indigenous peoples, gatherers, hunters, quilombolas communities and small farmers. Quilombola communities are ethnic groups, predominantly made up of black rural or urban population, descendants of former slaves, who define themselves

based on specific relations with the land, kinship, territory, ancestry, traditions and cultural practices (Instituto Nacional de Colonização e Reforma Agrária, 2019). They have been historically using these floodplains terrain for providing essential elements to their survival (water, food, transport) and their rights to dwell within these areas are protected by the legislation (Brasil, 1934), but the uncertainty about the land ownership is a major factor promoting conflicts between large farmers and these communities. Some of these communities as the quilombola community of Caraíbas near Pedras de Maria da Cruz, have even undertaken the task of defining the limits of their own territory to pressure the SPU to delineate the MOFL and defy large farms (Figure 2a). As result, the local association (*Associação dos Vazanteiros e Pescadores Artesanais da Ilha da Capivara e Caraíbas*) received from SPU an authorization term for the sustainable use (*Termo de Autorização de Uso Sustentável - TAUS*) of a 2000 ha area that warrants the community its use for housing, fishing and sustainable agriculture (Figure 2b). Although Brazil concentrates huge areas of rural land, it still has one of the worse record of land inequality (Wilkinson et al., 2012). Identifying government-owned lands on federal river banks will help, among other aspects, to recognise the rights of these traditional communities and reduce land conflicts. Some efforts have been made in the past by the Brazilian Government to define these marginal lands but were mostly considered unsuccessful. Some of these efforts have used geomorphological analysis and a digital elevation model (DEM) from the Shuttle Radar Topography Mission (SRTM) but did not achieve sufficiently accurate results. The very large extent of areas concerned and the lack of financial resources for acquiring high precision digital models are some of the limiting factors for the precise definition of these marginal lands.

The original Brazilian law did not establish clear criteria for defining marginal lands, which may be related to floodplains, but are not necessarily equivalent. For this task, the SPU was instructed to define a methodology to identify and delimit these areas. The agency adopted the MOFL approach by which an “average” flood line is calculated based on historical data. This

is currently the standard method for the whole of Brazil and is presented below in the Materials and Methods section. The method is a simple averaging approach excluding very short (≤ 3 years) and long (≥ 20 years) return periods (see below). It can be seen as a simplification of more common water gauge data analysis method using probability distribution function such as the Weibull equation, the Log-Pearson Type III frequency analysis or the Gumbel function (Gartner et al., 2016). Still, a major drawback of these approach lies on the assumption of stationarity of the data time series. In other words it assumes the invariance of the probability distribution function (Milly et al., 2008; Sivapalan & Samuel, 2009). Changes in the land cover and interferences in the water cycle through river damming or deviation of the river course for irrigation can invalidate the assumption of stationarity (Milly et al., 2008). At a longer time scale, changes in weather patterns can have the same effect (Coulibaly & Dibike, 2004). Methods have been proposed to detect trends in historical data to avoid the assumption of stationarity like the Copula bi-variate function that can adapt itself to longer trends (Kang & Jiang, 2019).

In our case, the method developed by the SPU had to be used in order to maintain a unique and simple approach that can easily be explained and applied in all SPU agencies across Brazil.

Within this context, our objective is to test a methodology using satellite image data paired with time series of river gauge data to delineate the MOFL with sufficient precision to determine the extent of the São Francisco River floods corresponding to the MOF calculated through the SPU method. For this, a 600 km reach of the São Francisco River between the Três Marias Reservoir and the Minas Gerais-Bahia border was chosen as a pilot project. Furthermore, because the year 2020 is the first flood year since 2012 we intend to compare the 2020 results with the last time when the MOF was attained and remote sensing data were available to match these dates. It was especially hoped that Sentinel-1 data could be used since being a SAR imager, it is ideal to capture scenes under frequent cloud cover which is typical during the wet season when high flood levels are more likely to occur.



Figure 2. The quilombola community of Caraíbas near Pedras de Maria da Cruz showing the mapping by auto-determination of the territory where they dwell (a). The TAUS Caraíbas is a territory that guarantees about 2000 ha of Union lands in a region marked by environmental and land conflicts (b).

The São Francisco floodplain project

For the São Francisco River, the MOFL was originally set to be defined by the floods of 1867. However, it was never effectively delineated. Since then, the natural hydrological dynamics of the river have caused changes in its banks, not to mention the many human interventions that have altered its original course (bridges, dams, retaining walls, etc.). This unresolved situation has resulted in many conflicts, dissatisfaction and lawsuits between dwellers, land owners and government instances (i.e. state, municipal) over issues such as taxes, responsibility, ownership rights and so on.

This peculiar situation of Brazil regarding floodplains and marginal land have brought the SPU to seek alternate approaches to delineate the MOFL using GIS and remote sensing technologies. It is in this context that we argue that establishing a direct relationship between hydrological data and satellite images can provide a much more efficient approach than the use of geomorphological or DEM data with a poor vertical precision (up to 5 m in the case of SRTM). The main rationale being that very specific locations are being sought and not some probability of flood or flood susceptibility. These locations have a legal aspect demanding a “binary” type result: inside and outside the MOFL.

The availability of imagery from a variety of optical and synthetic aperture radar (SAR) satellites allows to directly relate events corresponding to floods with the moment of image acquisition. In consideration to the extension of the Brazilian territory ($\approx 8.5 \text{ Mkm}^2$), the lack of financial resources and the absence of high precision topographic maps, remote sensing presents itself as the only viable approach to solve this issue.

MATERIAL AND METHODS

The implementation of this pilot project took place through a sequence of steps planned to progressively validate the approach idealized. The selection of the São Francisco River came naturally, being arguably the most important river of Minas Gerais which is the state at the origin of the initiative (SPU-MG). Firstly the SPU method of defining the floodplain was implemented in a Python program that read the in situ gauging station data and produced a Mean Ordinary Flood stage value as well as a list of dates in the past 60 years for which the level was reached. Given these dates, the image repositories are investigated to determine the usable images (number and quality) for all water gauge stations. The following steps consisted in finding the most consistent approach for extracting the water surface, transform the water mask in vector and build a mosaic of river sections of the MOFL. Finally, a validation method was chosen involving field work and hydrological analysis. These steps are illustrated in the flowchart of Figure 1.

The São Francisco River reach under study

With 2700 km, the São Francisco River is a strategic river in Brazil (Figure 3) and ranks 27th amongst the 32 largest rivers in the world (Best, 2019). It is the largest river to cross the semiarid region of Brazil over a distance of more than 1000 km for which it is the main source of fresh water. The seven hydroelectric dams of its course produce over 10 GW of electrical power (Agência Nacional de Águas, 2019). Its watershed is populated by over 12 million people, most of which are in Minas Gerais,

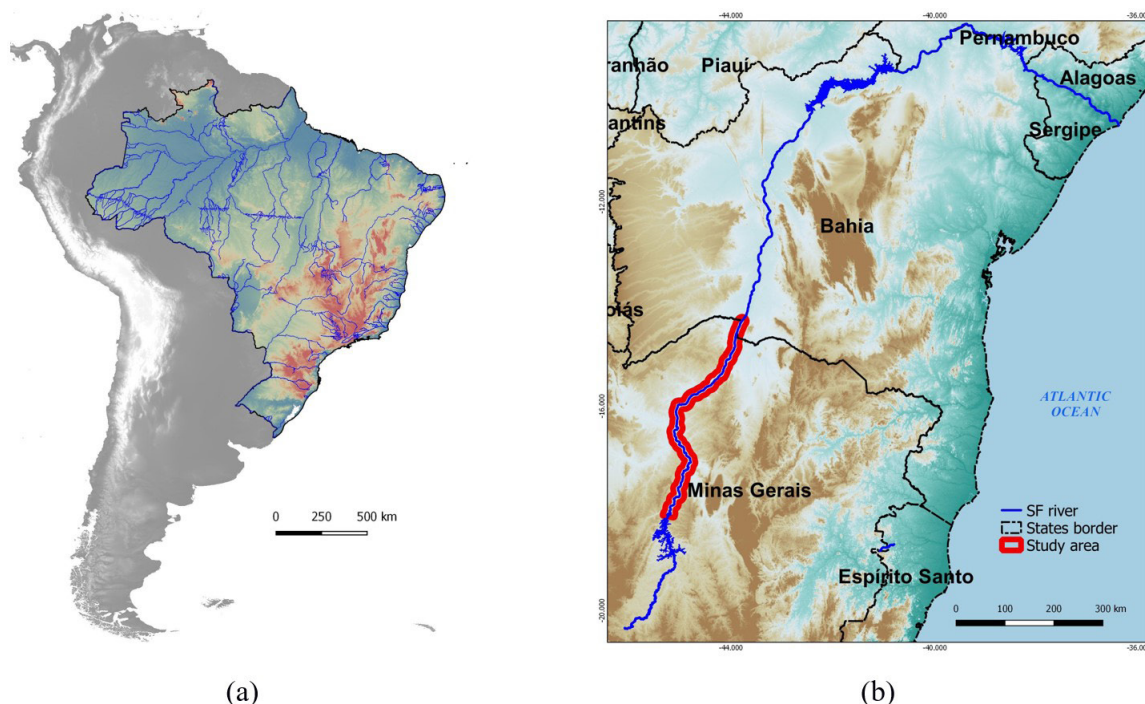


Figure 3. Rivers of the Federal domain in Brazil (a) and the São Francisco River crossing five Brazilian states and showing the river section under investigation (in red) (b).

the state where it has its source and through which it flows over about 1200 km. For this project, our focus is concentrated on a 600 km reach of the river between the Três Marias Reservoir and the border of Minas Gerais with the state of Bahia (Figure 3b).

The marginal lands of this reach are under the responsibility of the SPU/MG which initiated the project. No form of discharge control is applied to this section other than the Três Marias Reservoir at the upstream end. The northern portion of the section is particularly affected by frequent conflicts between large farms and small traditional communities because about 25% of the lands are considered unsettled by the Government (Instituto Brasileiro de Geografia e Estatística, 2006). Six rural settlements and one quilombola territory were created in the region bathed by this section of the river by the Federal Government through the land reform policy to provide land access to these communities (Instituto Nacional de Colonização e Reforma Agrária, 2020). However, these efforts are still insufficient. In 2017, 1168 conflicts were registered over land dispute in Brazil involving thousands of traditional population families (Paulon Girardi, 2019). Within the São Francisco floodplains, according to INCRA data, sixteen conflicts were registered in the seventeen quilombola communities identified involving area disputes, land conflicts and repossession actions that culminated in death threats, blocking access to the communities and armed conflict, among others.

In situ river gauge stations with daily readings are located all along the river course. Depending on the station, almost a century of observations of water stage is available through Brazil's National Water Agency (ANA). However, the older data may not necessarily reflect present hydrological conditions. On the one hand, contemporary floods have been known to be more severe for several reasons like recent floodplain obstructions, destruction of wetlands that used to retain floodwater, reduction of natural vegetative cover, imperviousness

of urban areas and global changes in weather patterns (Alfieri et al., 2017; Best, 2019). On the other hand, damming, water withdrawal (water pumping, irrigation) and transfer (canals) have had a tempering effect on most large rivers around the world (Gupta & van der Zaag, 2008). The São Francisco did not escape this fate, with a cascade of five major dams along its course and a huge water transferring project (Roman, 2017). It has seen its peak discharge at the mouth reduced by a factor of about 35% (Santos et al., 2013). The medium São Francisco (between Pirapora and the Sobradinho Reservoir) has seen its discharge regularised by the construction of the Três Marias Reservoir just upstream of Pirapora (station 41135000) whose construction started in 1957 and was inaugurated in 1962. Still, in 1979 the Três Marias dam was full and could not hold the waters causing one of the most severe floods ever recorded (Braga et al., 2012) that inundated many of the riverine cities and was characterised the third most destructive after the 1919 and 1926 floods (Brasil, 1980). Figure 4 shows three image portions of the same sector near Pedras de Maria da Cruz with three very different water stage situations including the 1979 flood (not at peak level).

In situ and remote sensing data

Historical time series from river gauge stations are used to report the water stage (or level) at different cross sections and to calculate the corresponding river discharge using a corresponding rating curve. A rating curve is built for each station (and periodically updated) that establishes the relation between the measured stage and the discharge. The rating curve is an essential tool for flood frequency analysis. In order to delineate the flooding area, the return period is often used as a measure of flood probability (Monmonier, 1997).

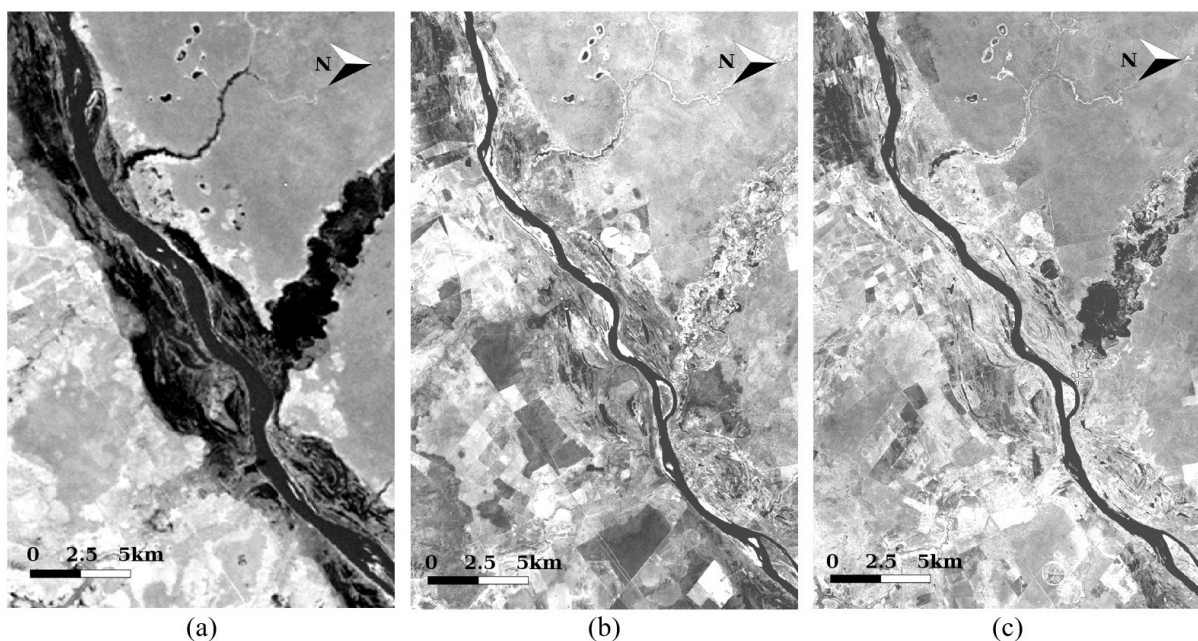


Figure 4. Comparing three situations of a section of the São Francisco River near station 44290002: in (a) the flood of 1979 (3-4 weeks after its peak) as seen by the MSS sensor of Landsat-2 (band 7); (b) the drought of September 2016; and (c) the flood (mild) of January 2020, both from the infrared band of Sentinel-2.

For this study we used a series of seven in situ hydrological stations (ISHS), some of which have water stage data since the 1930's. The location of these seven ISHS is illustrated in Figure 5. Table 1 shows some of the hydrological characteristics of these seven hydrometric stations. For the reasons mentioned above, we restricted our determination of the MOF to the past 60 years. It is also clear that in addition to the effects of climate change and natural hydrological dynamics (erosion, deposition, destruction due to floods, etc.), the dynamics of the land use / land cover might have had their role in affecting the hydrological parameters and the shape and size of the floodplains. That said, a period of 60 years was the trade-off we opted for between having a long enough time series of data and avoiding the effects of the dynamics of the land.

The remote sensing data was divided in two distinct periods: pre-2020 and 2020. The reason for this subdivision is that the project was initiated in 2018 which was in the midst of an eight years drought period that started in 2012. Prior to 2012, almost only (but not exclusively) Landsat images were systematically acquired and easily available. In 2020, the return of high waters and a regular flood made possible the use of Sentinel-1 and -2 images with a better spatial resolution and better revisit frequency.

Pre-2020 image bank

The São Francisco River receives most of its precipitation waters (> 80%) in the October—March period when the sky is often covered by clouds. This is a strong drawback for getting usable optical image data in these periods. The first criterion used to select image data was the acquisition date that had to correspond to one of the MOF water stage with a tolerance. The second criteria was the condition of cloud cover that had to be within reasonable proportion above the river channel. In addition to clouds, the atmospheric effect could hinder the water surface extraction. Images with at least long cloud-free sections of the river were selected. The following image bank platforms were searched: Earth Explorer (U.S. Department of the Interior, 2021), Alaska Satellite Facility (2021), Earthdata (National Aeronautics and Space Administration, 2021) and INPE-DGI (Instituto Nacional de Pesquisas Espaciais, 2021). These yielded images from the following satellite/sensors: Landsat-5,-7,-8/TM, ETM, OLI, Alos/Palsar, CBERS/MUX and ASTER/VNIR. By far, the Landsat images were the most usable because of their long historical data availability (1984—ongoing for the TM, ETM and OLI sensors), their systematic revisit period of 16 days and

their > 30000 km² per image coverage. Some of the other image types were used mostly to fill in gaps in the Landsat images caused by clouds and cloud shadows.

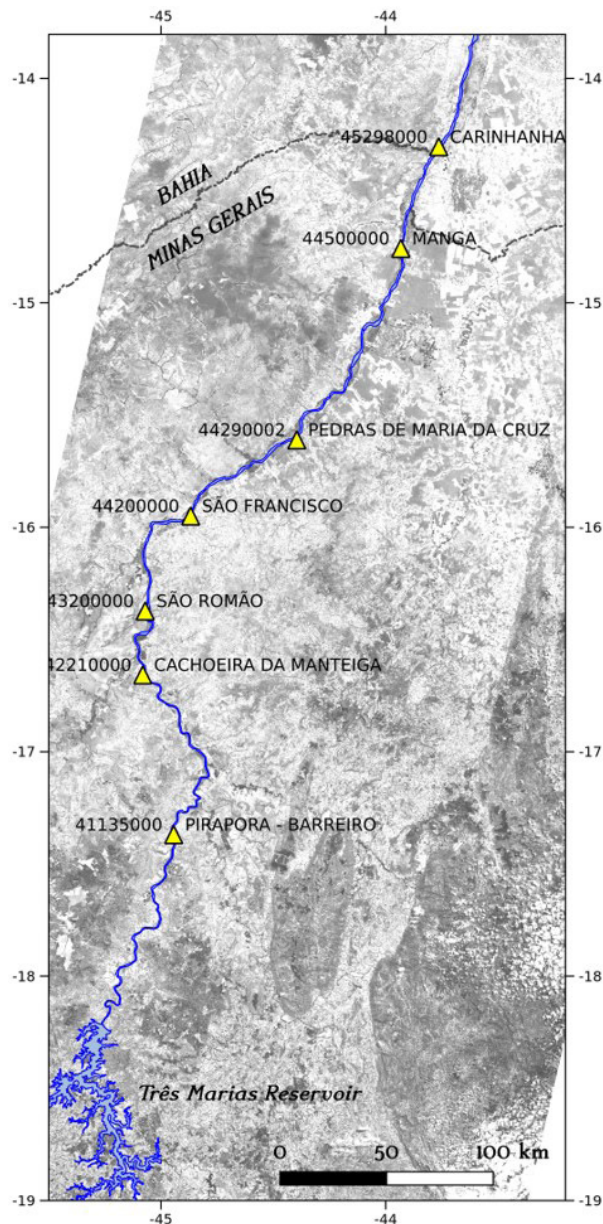


Figure 5. Location of the seven stations used in the study with a Sentinel-2 red band image as background.

Table 1. Some hydrological characteristics of the seven stations used in this study.

Station (ANA code)	Width av. (m)	Discharge av. (m ³ s ⁻¹)	Source at (km)	Drainage area (km ²)
Pirapora (41135000)	270	841	686	62101
C. do Manteiga (42210000)	367	1169	758	107000
São Romão (43200000)	376	1569	802	154000
São Francisco (44200000)	480	1808	843	184000
P. de M. da Cruz (44290002)	470	2017	909	195000
Manga (44500000)	425	1953	978	202000
Carinhanha (45298000)	550	2192	1098	254000

2020 image bank

The year 2020 started with precipitations in accordance with what normally happens this time of year breaking an eight years “drought”. These precipitations generated discharge levels compatible with the MOF levels. For this short period of two months we concentrated our image search to the two twin satellite constellations Sentinel-1 (S-1) and Sentinel-2 (S-2) from the European Space Agency (2021) Sentinel Datahub (European Space Agency, 2021). Because S-1 is a SAR system, it does not suffer interference from clouds and other atmospheric effects so that all images sensed are normally usable. The S-2 being optical can only produce usable images when the sky is clear so that few images were expected to be usable.

Mean ordinary floods calculation

The mean ordinary flood line (MOFL) is based first on calculating the mean ordinary floods (MOF) which is based on historical water stage data from hydrometric in situ stations. Instead of using the return period principle, the SPU adopted an approach that first extract the highest water stage of every hydrological year (October to September in Southeast Brazil) of all in situ stations within the river reach being considered. Then it excludes highly recurring floods (return period ≤ 3 years) as well as low frequency floods (return period ≥ 20 years). The remaining data is averaged to make up the MOF. The methods demands that at least 20 years of data be considered but more is highly desirable. Because it is highly unlikely that the date and time of an image will correspond exactly to the MOF water stage, a difference of a few centimetres is considered through a tolerance factor. Upon trials, it was found that a tolerance factor of ± 10 -15 cm enabled to find candidate images for all situations. With new satellite missions like Sentinel-1 and -2 having a return

time of 5 to 12 days, a smaller tolerance factor will eventually be sufficient.

Using data from the São Romão in situ station (43200000) we illustrate how the process is done:

1. The highest water stage is extracted from the 68 hydrological years (1 October—30 September) available (Figure 6);
2. The 68 records are ordered from the highest level to the lowest one (Figure 7);
3. Records with the lowest (≥ 20 years) and highest frequency (≤ 3 years) are discarded;
4. The remaining are averaged to calculate the MOF (9.40 m in this case)
5. The MOF water stage is transformed into an interval using the tolerance factor;
6. All dates for which the water stage falls within the interval are recorded and compared with the dates of the image dataset records;
7. The images corresponding to these dates are pulled and check for quality (atmospheric conditions and other defects);
8. The images are processed to extract the water surface;
9. The water surface images are transformed in vector format and cleaned.

Figure 6 shows an example of where the MOF is situated (9 out of 24837 days or about 0.36% of the time) with relation to the absolute frequency of water stages during the 68 years of record. It can be observed from inspecting Figure 6 that the period between 2012 and 2019 is characterised by the absence of important flood events. This was unfortunate for the second phase of the project since we could not take advantage of the Sentinel-1 and -2 image banks (the first Sentinel was launched in 2014) with a high resolution (10 m for S-1 and 10-20 m for most S-2 bands) and short revisit time (5-12 days).

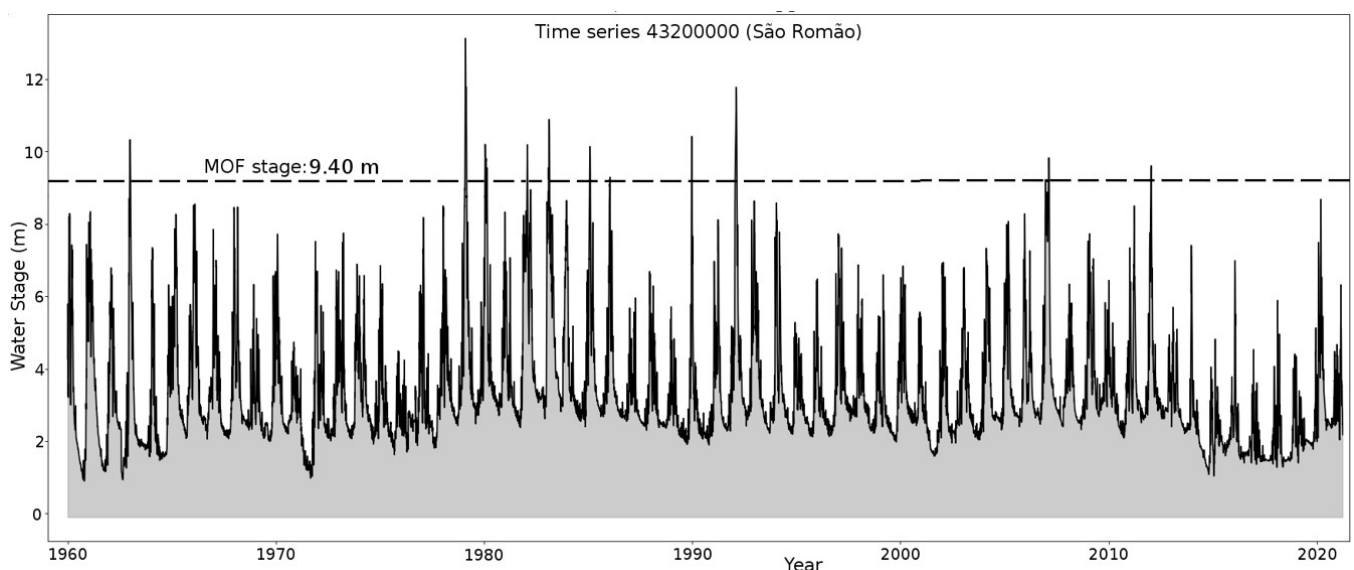


Figure 6. Water stage time series for the 43200000 in situ station (São Romão). Note how the MOF has not been reached since 2012 but came close in 2020.

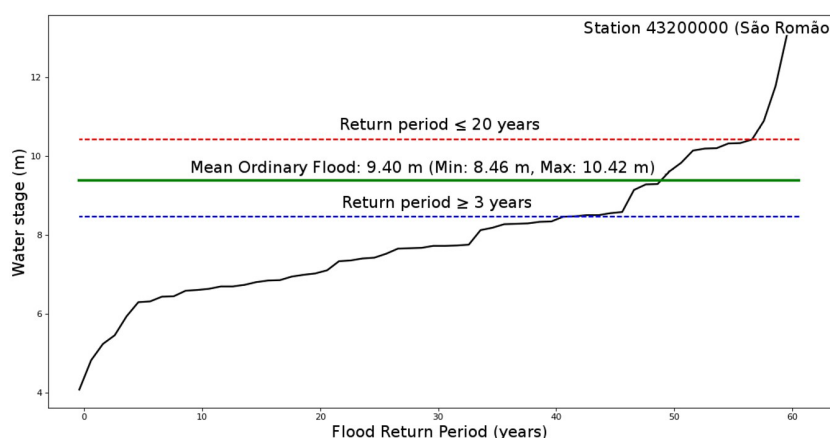


Figure 7. Calculation of the water stage corresponding to the Mean Ordinary Floods (green line) against the observed flood return period.

Water surface extraction from remote sensing data

The extraction of the water surface using the near (NIR) and shortwave infrared (SWIR) bands of satellite images is one of the most straightforward application of remote sensing technology (Barrett & Curtis, 1982; Smith, 1997; McCoy, 2005). The early work by Work & Gilmer (1976) using Landsat-1 MSS images for mapping ponds and lakes is one of the first published work addressing this issue. This cause of effect is due to the fact that almost all radiation in the NIR and SWIR parts of the spectrum are absorbed by water which reflects almost no radiance to the sensor (Ji et al., 2009; McCoy, 2005). Later, with the launch of SAR satellites the same statement is valid since SAR images usually permit the easy separation of land and water. Except in very windy conditions causing the presence of waves, the microwave impulses of a SAR instrument are reflected away from the antenna in side-looking imaging systems making water appear black (low energy echos) in these images (Lewis, 1998). Amongst the various methods to extract the water surface from optical remote sensing data, the most common are multispectral classification or segmentation methods (Lira, 2006), and threshold of a single band (Jain et al., 2005) or the use of indices like the normalised difference water index (NDWI) proposed by McFeeters (1996) or some variation of it (Xu, 2006). Likewise, SAR data was often perceived as a more viable alternative to optical data for their ability to penetrate cloud cover and not depend on solar illumination of the scene to record back-scattering data (Slater et al., 2006; Brisco et al., 2009). In order to create the MOFL, we opted to examine images from five missions involving eight satellites: Sentinel-1A and -1B, Sentinel-2A and -2B, Landsat-5 and -8, CBERS-2 and Alos-1. We tested different data types, spectral bands and classifying algorithms in order to find the best compromise between simplicity, efficiency and quality of results to separate the water class from other types of land cover. To evaluate the best procedure we used an approach based on the differences in area and geometry between the results obtained and the water surface reference map produced from visually interpreting multispectral images from the Dove imager (Planet Labs Inc.) with a 3 m spatial resolution. The results of these tests are presented in two publications, the results of which can be found in Pôssa & Maillard (2018) and Maillard et al. (2018)

and are summarised in Appendix A. Following the conclusions of these studies, all optical image data was classified using the K-means segmentation algorithm while all SAR data was classified using the Support Vector Machine (SVM) algorithm.

Validation of water surface delineation

MOFL Accuracy: Once chosen the best method for separating and delineating the water surface and producing the MOFL for the whole extension of the reach, our next step was to assess in the field the accuracy of the line obtained. Considering over 1000 km of MOFL (both sides of the river) and the limited financial resources and time, only a limited amount of checking was permitted. We opted for sampling areas more susceptible to errors. In steep banks, the increase in water stage does not involve an important increase in the area (or width) occupied by the river. However, in floodplains, subtle rises in the water stage could be translated into large flooded areas so that these areas were prioritized.

The method used to identify the MOFL on the terrain is based on the knowledge of its vertical position and required a topographic profile. The precise elevation value of the MOFL can only be determined near the river gauge stations with known elevation reference. Conversely, the areas between stations can only be the result of an interpolation and therefore present only limited precision. A precise geodetic survey was done using two Global Navigation Satellite System (GNSS) receivers to create a series of six topographic profiles near four of the river gauge stations in floodplain situations to establish 1) the true location of the MOFL, 2) the location of the MOFL found on the day of the satellite image and 3) compare it with the location determined using the satellite image itself.

Topographic survey: To produce the topographic validation profiles, we combined the measurements of three instruments: a geodetic GNSS, an optical level and a laser range finder. The GNSS was used to survey the start and end points along with some middle points (where angles were needed). The optical level measured the elevation difference every 20-30 m between GNSS survey points and the laser rangefinder was used to measure the distance between these intermediate points. Figure 8 shows the method

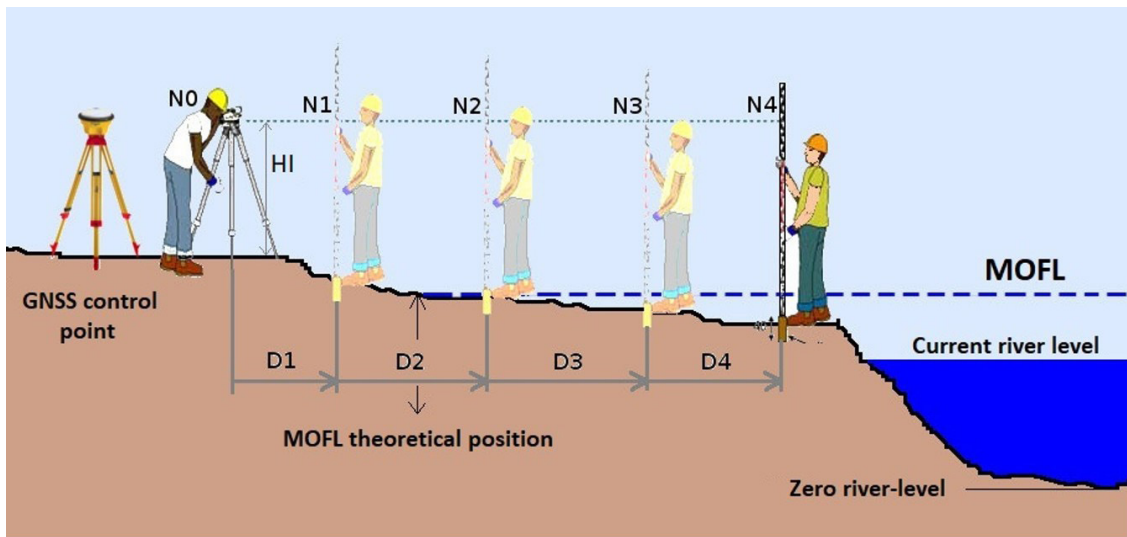


Figure 8. Illustration of the concept of profile survey from an optical level and a precision GNSS station. Where N is the measurement point, D is the distance between the points and H is the height of the instrument.

Table 2. List of stations with their relative Mean Ordinary Floods stage, the corresponding satellite image, the water stage at the image date and the stage difference between the two stages.

Station name	km from source	Elevation (m)	Image date	Satellite	Stage at image (cm)	MOF stage (cm)	Difference (cm)
Pirapora	666	469.38	18/02/2007	CBERS-2	336	377	-41
C. do Manteiga	780	447.49	19/12/2006	Landsat-5	949	952	-3
São Romão	819	443.85	18/02/2007	CBERS-2	954	940	+14
São Francisco	884	437.90	08/02/1985	Landsat-5	965	983	-18
P. de M. da Cruz	948	432.06	08/02/1985	Landsat-5	899	883	+16
Manga	1070	420.70	08/02/1985	Landsat-5	894	838	+56
Carinhanha	1124	416.91	08/02/1985	Landsat-5	761	728	+33

used for collecting the profile points. In the example, note that the reference GNSS is positioned outside the LMEO identified from the satellite images, and that the profile is drawn up to a point that is guaranteed to be within the MOFL.

The measurements obtained from the optical level were interpolated at each meter in order to obtain better accuracy and to be able to match this information with the profile path, which was also interpolated at each meter. As the river level on the day of the survey was known and the GNSS base was located at the level reference (LR) of the nearest river gauge station, it was possible to determine the theoretical elevation of the MOFL and its position along the topographic profile. This position was then compared with the position extracted from the satellite image used in each sector surveyed.

RESULTS AND DISCUSSION

The MOF and the corresponding images

Table 2 shows the result obtained for the seven river gauge stations within the São Francisco reach along with the images that were found having the closest water stage. The difference between

the two stages is also shown. Four stations were related to three Landsat-5 images (same orbit/date) of February 1985 which surpassed lightly the MOF stage in three cases. Cachoeira do Manteiga was coupled with a Landsat-5 image of 2006 and the remaining two stations (Pirapora and São Romão) were coupled with two CBERS-2 Images of 2007. The difference in water stage should be examined from a spatial extent stand and will be considered in the validation sub-section below. It is noteworthy that the MOF is different for every station and occurs at different dates as the celerity (flood wave speed) dynamics affects the propagation of the water.

Figure 9 illustrates well that the flood peak of January 2012 took about nine days to cover the distance between Cachoeira do Manteiga and Carinhanha representing about 350 km. During the dry season, this time gap is about 15 days.

The year 2020 marked the end of a long “dry” period of seven years (2012-2013 through 2018-2019) including the year 2014 which caused a serious water crisis in Southeast Brazil (Nobre et al., 2016). Although some floods were registered along the São Francisco River, the water stage did not reach the MOF stage as shown in Table 3. Only the Pirapora section could be used with a small difference between the MOF stage and the stage at the image acquisition time of 15 cm. Other possibilities with small stage difference are all attributable to optical images (Sentinel-2 or Landsat-8) with important cloud cover (40-68%).

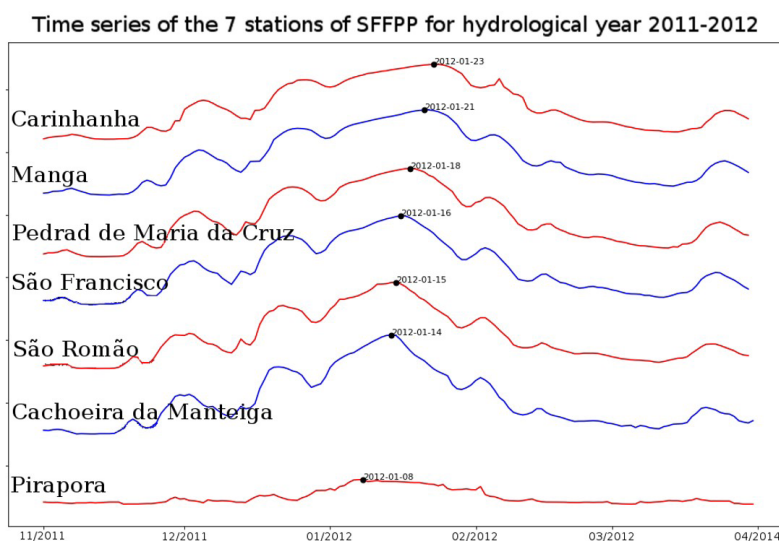


Figure 9. Graph illustrating the peak flood period between Pirapora and Carinhanha for the hydrological year 2011-2012. Note the 1–2 days difference between most stations for the flood to reach. The Pirapora station appears to stand out as a clear peak is not visible. The vertical scale has been altered by an increase of 10 m between stations to ease visualization.

Table 3. List of maximum stage for the seven fiovietrometric stations on the São Francisco reach with the closest satellite image found, the corresponding stage and the stage difference to the MOF.

Station	Maximum 2020 stage (cm)	Max. stage date	Image date	Stage at image date (cm)	Image type	Difference from MOF (cm)
Pirapora	394	2020-03-08	2020-03-05	362	S-1	-15
C. do Manteiga	900	2020-03-09	2020-03-10	899	S-1	-53
S. Romão	851	2020-03-10	2020-03-10	851	S-1	-89
S. Francisco	890	2020-03-10	2020-03-10	890	S-1	-93
S. Francisco	890	2020-03-10	2020-03-12	885	S-2*/L-8**	-98
P.M.Cruz	864	2020-03-10	2020-03-05	770	S-1	-113
P.M.Cruz	864	2020-03-10	2020-03-12	861	S-2*/L-8**	-22
Manga	816	2020-03-13	2020-03-17	720	S-1	-118
Manga	816	2020-03-13	2020-03-12	814	S-2*/L-8**	-24
Carinhanha	NA	NA	2020-03-17	?	S-1	?
Carinhanha	NA	NA	2020-03-12	?	S-2*/L-8**	?

S-2*: Sentinel-2 image with an average of 40% cloud cover; L-8**: Landsat-8 image with an average of 68% cloud cover.

Even considering the 35 years passed since the 1985 Landsat images, they were still the best set of images to define the MOFL.

Water surface images

A number of considerations had to be taken to transform the binary “water—no water” image into the MOFL. The correspondence between the MOF stage and the image date stage were never exactly the same. The MOF stage was usually inserted between a lower and a higher stage with the water either rising or receding. In the case of receding water, it could be expected that some areas were filled with water which had not enough time to infiltrate or evaporate. These areas should not be included within the MOFL. Figure 10 shows how the stage at the date of the image relates to the MOF and whether the water was rising or receding for six river gauge stations. In Pirapora (10a) and Cachoeira do Manteiga (10b) the water

stage is relatively stable but clearly below the MOF level for Pirapora. In São Romão (10c) and São Francisco (10d), the waters are receding but slightly above the MOF in the first case and below in the second one. In both Manga (10e) and Carinhanha (10f) the date of the image is close to the peak of the flood but well above the MOF (56 cm in the case of Manga, the largest gap). The differences in water stage are significance through the planimetric distance they represent in the field. This particular aspect is analysed below in the validation section.

The result for a section (in this case the widest of the reach we studied) is shown in Figure 11. Some smoothing was applied to the resulting MOFL to simplify unnecessary details caused by the resolution of the Landsat image (pixelated appearance). For each map produced, the images used with the date, the stage, the difference with the MOF stage and special considerations are clearly indicated (such as manually interpolated sections due to haze or small clouds). The data itself were saved in vectorial format (*shapefiles*).

Challenges of defining the floodplain through the “mean ordinary flood line” approach using remote sensing in Brazil: a case study of the São Francisco River

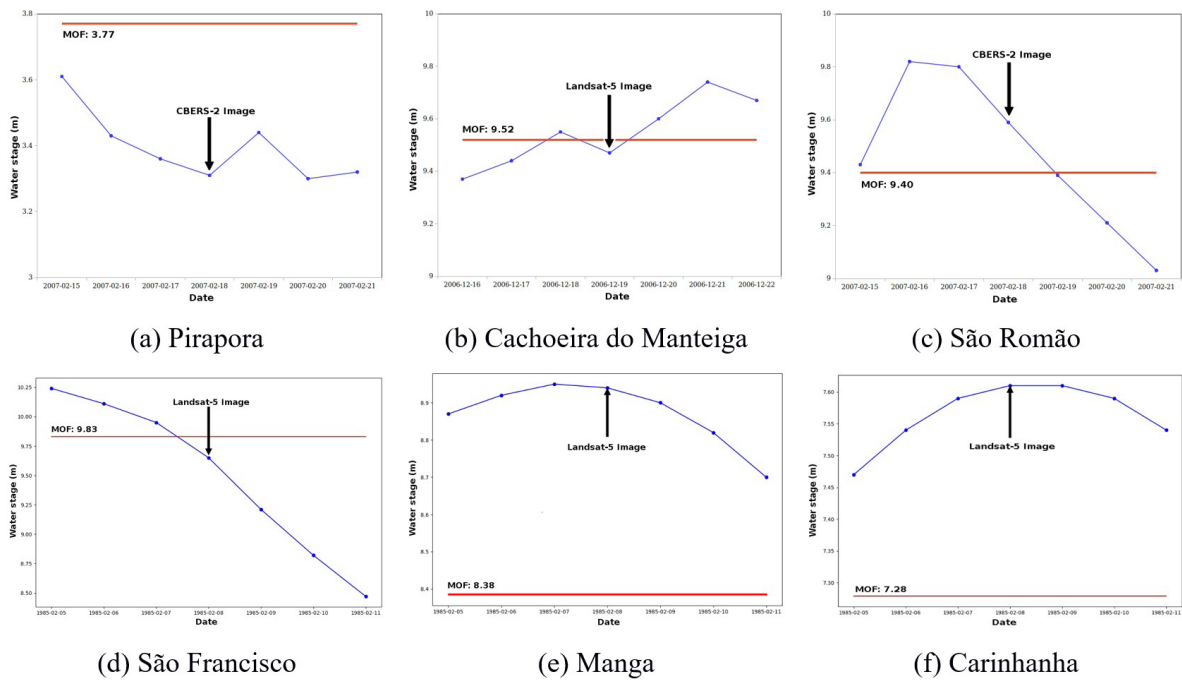


Figure 10. Six graphs showing the relative position of the water stage at image acquisition and compared with the MOFL stage. The position with relation to whether the waters are rising or receding can have an impact on the final MOFL.

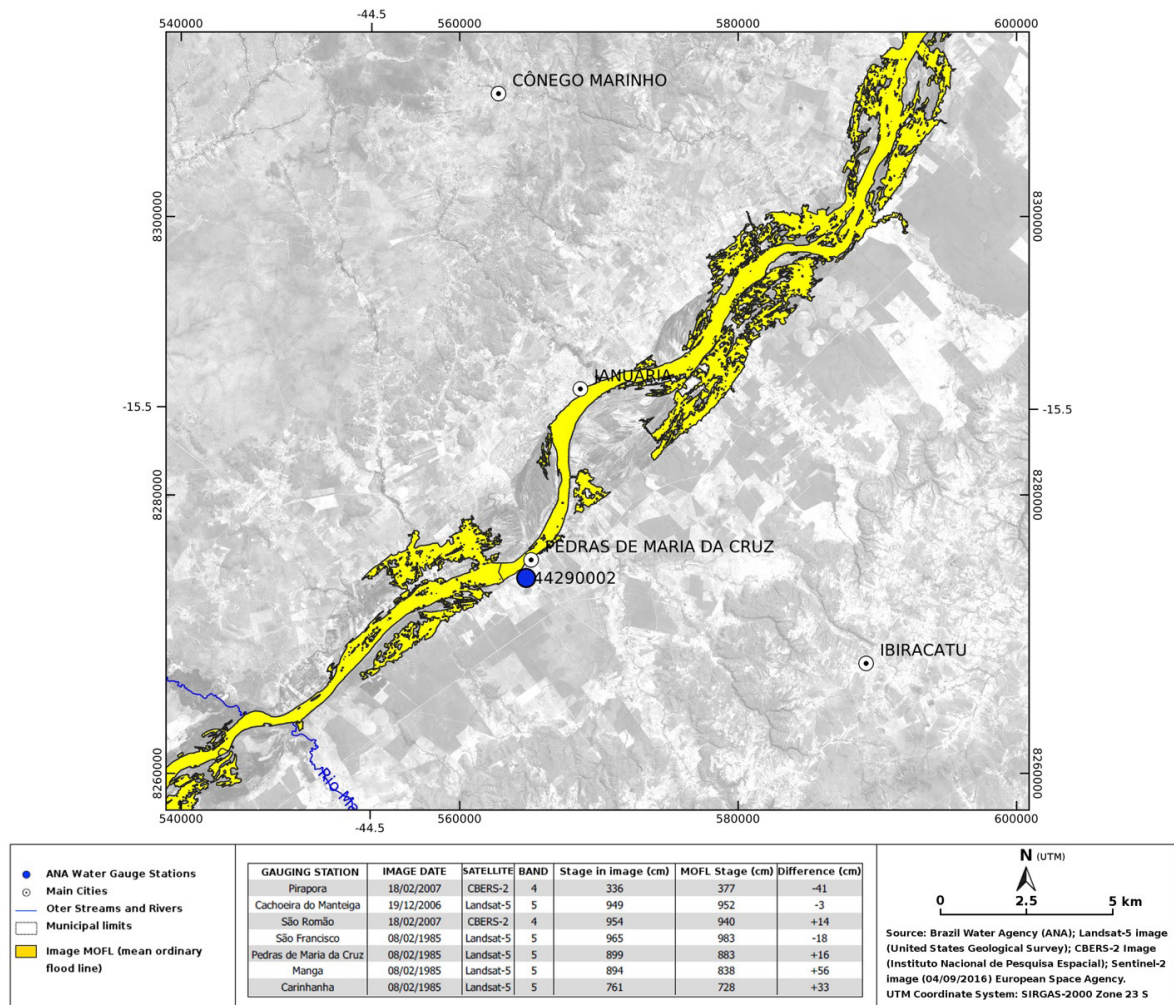


Figure 11. Example of one of the final map (portion) produced by the project team to serve as reference for the “Mean Ordinary Flood Line”.

Field work and validation

We chose to do the validation on a few selected sites to determine the suitability of our approach and its level of accuracy. The sites were selected on the basis of three criteria. First it had to be near one of the seven river gauge stations for which we had good accuracy over the true position of the MOFL having local water stage information. Second, the sites should be located preferably where the estimated MOFL arises doubt through a peculiar shape or location. Finally we chose sites where access did not pose any special difficulty as we needed to have a relatively clear line of site between the points that would form the topographic transects.

Five sites were selected covering the Pirapora – Januária section of about 300 km. For each site three lines were compared: the true MOFL location based solely on the water stage station data, the estimated MOFL based on the water stage corresponding on the image date and the actual (or final that represents the product delivered) MOFL we produced based solely on the classified images. All three lines are presented both vertically (in transects) and horizontally (against a Sentinel-2 false colour image) in Figures 12 and 13. These topographic profiles give a good idea of how the vertical difference between the three versions of the MOFL affect the horizontal shift. These shifts are better depicted in Figure 13.

Of the five sites, only one (Pedras de Maria da Cruz) did not cross the true MOFL which ended up located right on the edge of a small cliff we were not able to reach on the field. The first site (left bank of Pirapora) was special as it was selected because it crossed the MOFL twice within about 100 m. In all cases, the MOFL based on the classified image are lower than the true MOFL and, hence cover a smaller area between the two river banks than the true MOFL. This is somewhat desirable since it reduces the risk of conflict.

In all situations but the right bank of the Pirapora site, the MOFL based on the classified image is within one to three Sentinel-2 pixels (10 m to 42 m considering a diagonal setting) which was considered very good given that the MOFL was mostly based on Landsat-5 images with a 30 m resolution. It was attempted to cross the MOFL twice on the São Francisco site but it did not happen and was only discovered once the GNSS processing was done. Still the image-based MOFL appears within about 30 m.

Table 4 shows the accuracy obtained for the six sites including the Pirapora left bank double site. The table shows

three distances: 1) from the true MOFL to the MOFL based on the image date (Estim.), 2) from the MOFL based on the image date to the MOFL based on the classified image (Image) and 3) from the true MOFL to the MOFL based on the classified image. The result suggests that the stage difference between the true MOFL and the MOFL corresponding to the image date is quite small with an average of less than 5 m. On average both the distance between the true MOFL and the other two versions is less than 25 m with a peak value of 42.7 m in the case of the São Francisco site. Still, considering the atypical situations of these sites, these values were considered reasonable and completely usable for delineating the marginal lands under federal policy.

The use of only five sites for validation imposes some restriction as to the accuracy of the approach presented and it was discussed that such validation should probably be much more thorough through the acquisition of a high accuracy lidar survey. Our validation method also leaves unresolved the question of the MOFL passing through forested land that could perhaps benefit from the use of radar images that can better sense flooded areas in the understory. Still, at this point, the approach instigated can help solve many conflicts in the more disputed agriculture and pasture lands.

These results also suggest that the water stage tolerance should be in accordance with the geomorphological attributes of the river banks with higher tolerance in steep banks (i.e. ≈1 m) and low values in floodplain situations (i.e. <50 cm). The slope of the water surface is another criterion that should help to select a tolerance value. In the case of this particular reach of the São Francisco the water surface slope is about 10 cm/km on average. As a comparison, the slope of the Amazon between Manaus and the mouth is around 2-3 cm/km which would suggest a lower tolerance in terms of water stage difference between the MOF at image date and the true MOF.

Reflections on the MOFL

Our study showed the existence of a clear dry phase between 2013 and 2019 in the Minas Gerais portion of the São Francisco. Even the 2020 floods did not reach historical water stages corresponding to the MOFL. This same conclusion was also outlined by Santos et al. (2020) for a portion of the lower São Francisco basin that showed an important reduction of the surface area occupied by bodies of water along the São Francisco main channel they characterise as

Table 4. Accuracy estimates at six validation stations showing the difference in water stage between the MOF and the image date (column 2, 3 and 4) and the planimetric distances between the true MOF (measured in the field: True) and the MOF estimated corresponding to the image date (Estim.) and the actual MOF estimated through the image classification (Image). All sites are on the right bank except the first two marked LB.

STATION	WATER STAGE (cm)			PLANIMETRIC DIFFERENCE (m)		
	Image date	MOF	Difference	Image vs True	Estim. vs True	Estim. vs Image
Pirapora LB1	336	377	-41	20.5	8.9	11.2
Pirapora LB2	336	377	-41	16.0	20.2	4.3
Pirapora	336	377	-41	32.1	23.3	8.3
São Francisco	899	883	+16	30.9	42.7	2.1
P. M. da Cruz	899	883	+16	28.0	28.0	0
Januária	965	983	-18	17.1	19.2	1.9

Challenges of defining the floodplain through the “mean ordinary flood line” approach using remote sensing in Brazil: a case study of the São Francisco River

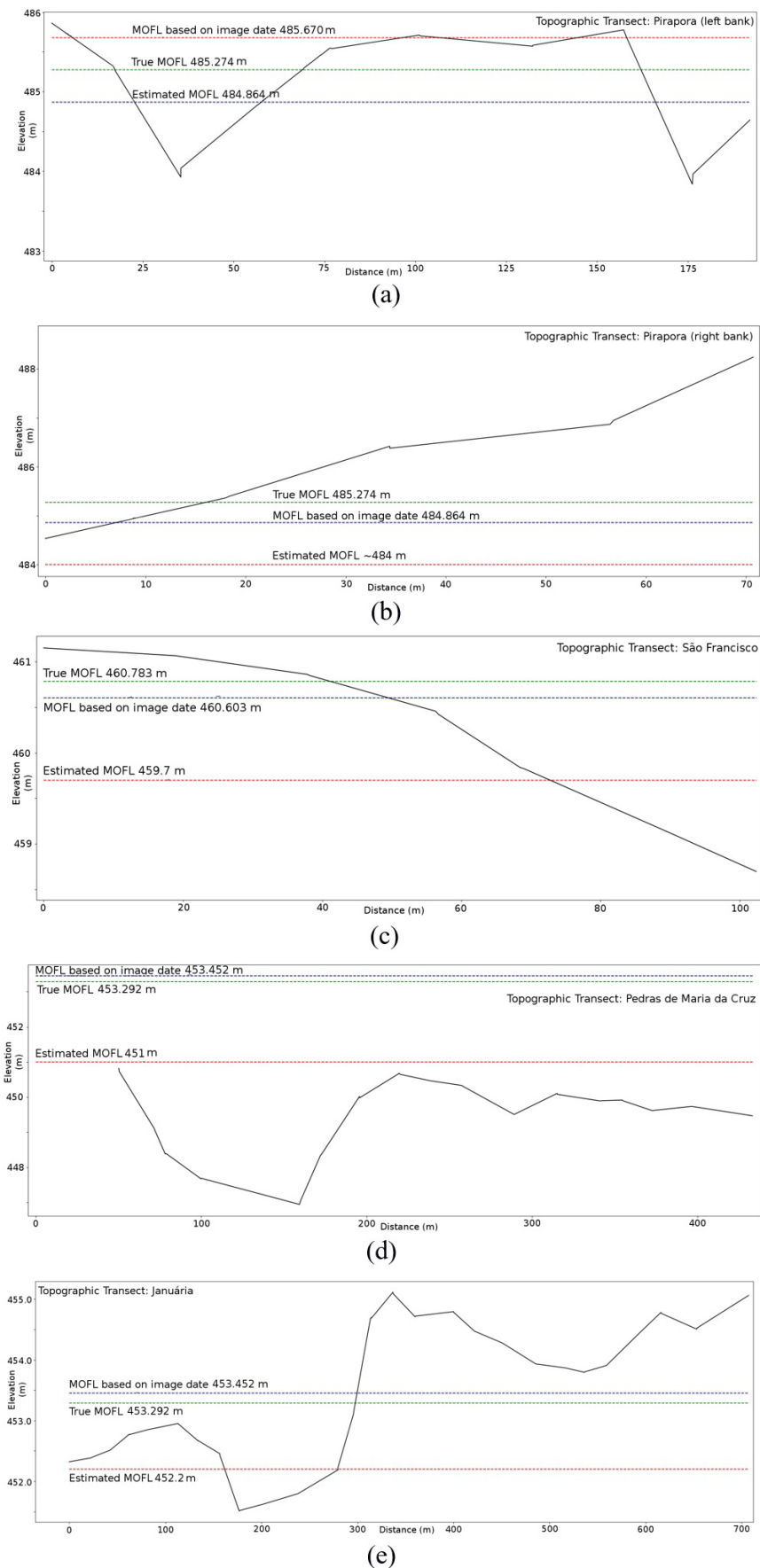


Figure 12. Five topographic transects carried out in the field using a geodetic GNSS and an optical level to validate the MOFL produced from the classified satellite images.

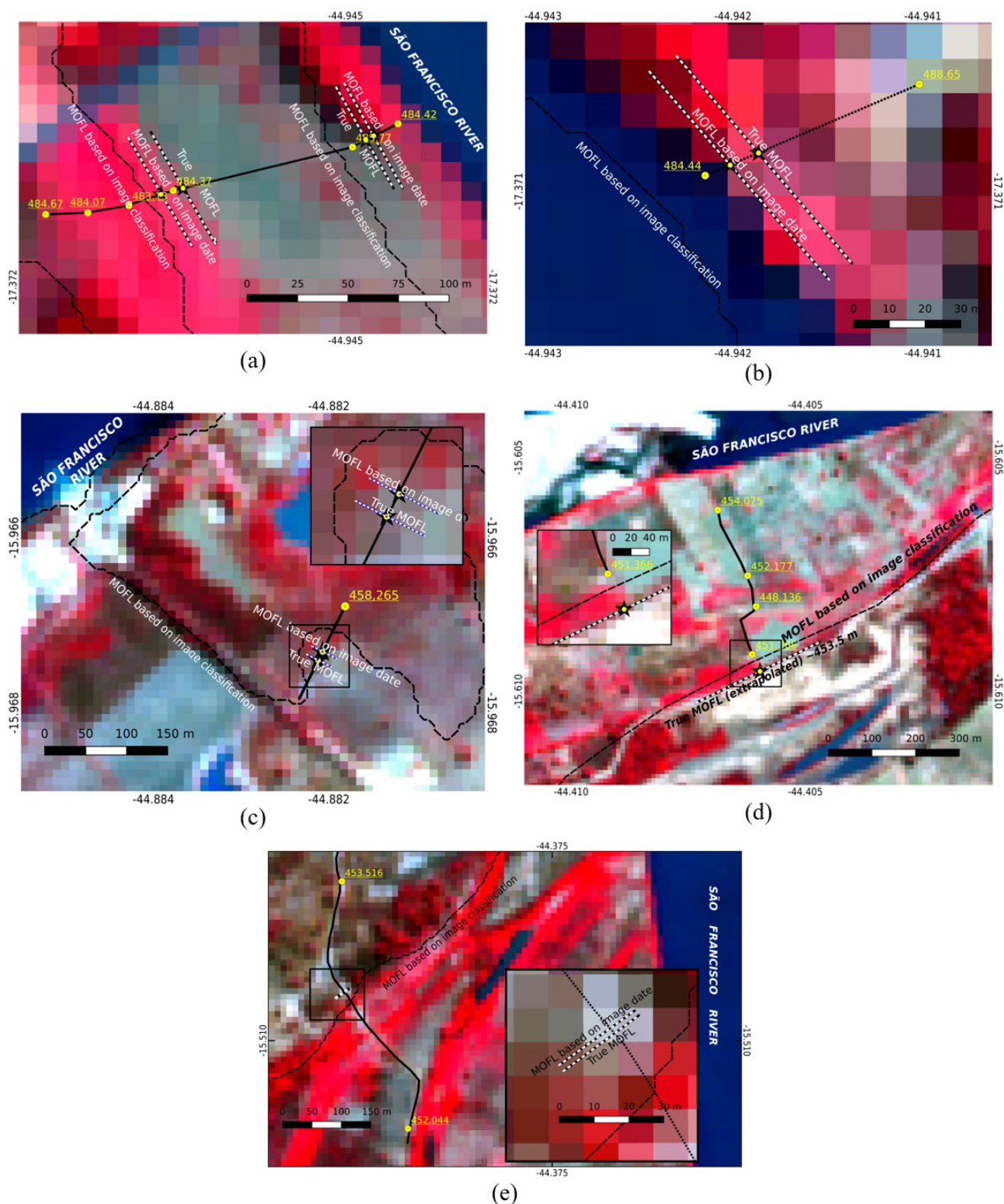


Figure 13. Planimetric visualization of the five topographic transects carried out for the validation of the MOFL produced from the classified satellite images. The background image is a Sentinel-2 image of October 2016 in false colour configuration.

land degradation and risk of desertification. Their study used a land vulnerability index (LVI) that combined two remote sensing products, the NDVI (normalised difference vegetation index) and NDWI (normalised difference water index). The former to

determine the portion of exposed land and the latter to identify areas covered by water. They conclude that the lower São Francisco has a high to very high vulnerability to land degradation and faces risk of desertification. In another recent study by Paredes-Trejo et al.

(2021), the author evaluated extreme drought events for the period 1980-2013 and found that drought conditions were worsening in terms of coverage, duration, and severity for the 1980-2015 period.

These observations bring forth the question of the effectiveness of the MOFL in the long term. The legal and technical aspects of the MOFL make it difficult to be revised over short periods of time. If a drying trend could be observed in less than 40 years (Paredes-Trejo et al., 2021), should the MOFL be based on a shorter period of analysis? Given these trends, can the land within the MOFLs be sustainably exploited or will over-exploitation threaten even more the land of degradation and desertification?

Conversely, the MOFL could become a management tool to promote revitalization of the river banks and floodplain in concert with the communities and the River Basin Committee. It has been pointed out that the River Basin Committee tends to prioritize such revitalization programs instead of large infrastructure programs like dams and transposition (Alves da Silva Rosa et al., 2021).

It is hoped that the implementation of the MOFL will dampen unsustainable situations of conflicts that have poisoned social relations between government, small communities and farmers but also that it will bring environmental benefits in view of the land degradation affecting the São Francisco River.

CONCLUSIONS

By combining hydrological data from in situ river gauge stations with satellite images from different missions we developed a method through which we were able to delimit a portion of the floodplain of the São Francisco River that carries a special legal significance: the Mean Ordinary Flood Line or MOFL. Land delimited by the MOFL is under the responsibility of the Brazilian Federal government that uses it as a tax collection instrument but also as a means to protect local traditional communities that dwell on it and extract their livelihood from it. Past attempts to delineate the MOFL were unsuccessful because of their slow pace and lack of precision. High resolution digital elevation models are not available in rural Brazil and other data source (SRTM, GDEM) are too imprecise. By calculating the MOFL at different river gauge stations and making a record of all past dates when the flood level was reached we retrieved historical satellite data corresponding with these dates. A water stage tolerance was included to be less restrictive. Maps of the MOFL were produced for the whole river reach. A field survey of some sections presenting some difficulty yielded an average positional accuracy of 24 m. A more thorough validation campaign was eventually planned but could not be carried out until the time of this manuscript.

Because the São Francisco River had been suffering from a long drier phase (2012-2020), more advanced satellite images from the two high resolution Sentinel constellations (-1 and -2) could not be used. Future MOFL projects should however give preference to these satellites mission and other missions like ALOS which might be more suited for regions with dense forest cover. The success of the approach relies on the in situ water stage stations and their recent decline in Brazil and worldwide (Calmant & Seyler, 2006) can strongly impair its application.

Once implemented, the MOFL will help avoid many social conflicts that the present unsolved situation has generated. The SPU is now in the process of expanding the São Francisco

pilot project to other parts of the country. At the end of this pilot project, a group of 16 SPU employees participated to a one week course on the method to determine the MOFL so that they can promote it in their respective region.

ACKNOWLEDGEMENTS

This project was instigated and financed entirely by the Superintendência do Patrimônio da União em Minas Gerais (SPU/MG) through a decentralised execution term (Process 23072.053550/2017-30 N° 1/2017) for research celebrated between the SPU/MG and the Geoscience Institute of Universidade Federal de Minas Gerais (IGC/UFMG). The authors are most grateful to the National Air and Space Administration (NASA), the United States Geological Survey (USGS), the Instituto Nacional de Pesquisa Espacial (INPE), the European Space Agency (ESA), Planet Labs Inc., ANA and the Serviço Geológico do Brasil (CPRM) for making available the wealth of image and data necessary for the execution of this project.

REFERENCES

- Agência Nacional de Águas – ANA. (2019). *Conjuntura dos recursos hídricos no Brasil: Informe anual* (Technical report). Brasília.
- Alaska Satellite Facility. (2021). Retrieved in 2021, September 15, from <https://asf.alaska.edu/>
- Alfieri, L., Bisselink, B., Dottori, F., Naumann, G., de Roo, A., Salamon, P., Wyser, K., & Feyen, L. (2017). Global projections of river flood risk in a warmer world. *Earth's Future*, 5(2), 171-182. <http://dx.doi.org/10.1002/2016EF000485>.
- Alves da Silva Rosa, L., Morais, M., & Saito, C. H. (2021). Water security and river basin revitalization of the São Francisco river basin: a symbiotic relationship. *Water*, 13(7), 907. <http://dx.doi.org/10.3390/w13070907>.
- Ávila, A., Justino, F., Wilson, A., Bromwich, D., & Amorim, M. (2016). Recent precipitation trends, flash floods and landslides in southern Brazil. *Environmental Research Letters*, 11(11), 114029. <http://dx.doi.org/10.1088/1748-9326/11/11/114029>.
- Barrett, E. C., & Curtis, L. F. (1982). *Introduction to environmental remote sensing* (2nd ed.). London: Chapman & Hall.
- Bartiko, D., Oliveira, D. Y., Bonumá, N. B., & Chaffe, P. L. B. (2019). Spatial and seasonal patterns of flood change across Brazil. *Hydrological Sciences Journal*, 64(9), 1071-1079. <http://dx.doi.org/10.1080/02626667.2019.1619081>.
- BBC News. (2021, 16 de julho). Europe floods: at least 120 dead and hundreds unaccounted for. *News*. Retrieved in 2021, July 17, from <https://www.bbc.com/news/world-europe-57858829>.
- Best, J. (2019). Anthropogenic stresses on the world's big rivers. *Nature Geoscience*, 12(1), 7-21. <http://dx.doi.org/10.1038/s41561-018-0262-x>.

- Bogo, R. S. (2020). Participatory master plan, territory and floods in Rio do Sul/State of Santa Catarina. *Cadernos Metrópole*, 22(48), 555-578. <http://dx.doi.org/10.1590/2236-9996.2020-4810>.
- Braga, B. P., Gondim Filho, J. G. C., von Borstel Sugai, M. R., da Costa, S. V., & Rodrigues, V. (2012). Impacts of Sobradinho Dam, Brazil. In A. K. Biswas, D. Altinbilek & C. Tortajada, (Eds.), *Impacts of large dams: a global assessment* (pp. 153-170). Berlin: Springer. http://dx.doi.org/10.1007/978-3-642-23571-9_7.
- Brasil. (1867, 30 de setembro). Lei nº 1.507, de 26 de setembro de 1867. *Coleção de Leis do Império do Brasil*, Brasília. Retrieved in 2018, April 10, from http://www.planalto.gov.br/ccivil_03/leis/lim/LIM1507.html
- Brasil. Câmara dos Deputados. (1868). Decreto nº 4.105, de 22 de fevereiro de 1868. *Coleção de Leis do Império do Brasil*, Brasília. Retrieved in 2018, April 10, from <http://www2.camara.leg.br/legin/fed/decret/1824-1899/decreto-4105-22-fevereiro-1868-553319-publicacaooriginal-71152-pe.html>
- Brasil. (1934, 20 de julho). Decreto nº 24.643, de 10 de julho de 1934. *Diário Oficial [da] República Federativa do Brasil*, Brasília. Retrieved in 2018, May 6, from http://www.planalto.gov.br/ccivil_03/decreto/D24643compilado.html
- Brasil. (1980). *Relatório de avaliação do impacto da cheia de 1979 na bacia do Rio São Francisco*. Brasília.
- Brasil. (1988, 5 de outubro). Constituição da República Federativa do Brasil. *Diário Oficial [da] República Federativa do Brasil*, Brasília.
- Brasil. (2012, 18 de outubro). Lei nº 12.727, de 17 de outubro de 2012. *Diário Oficial [da] República Federativa do Brasil*, Brasília.
- Brasil. Ministério da Economia. Secretaria de Patrimônio da União. (2019). *Terrenos e acrescidos de marginal de rio*. Retrieved in 2019, September 27, from <http://www.planejamento.gov.br/assuntos/gestao/patrimonio-da-uniao/bens-da-uniao/margens-de-rios>
- Brázdil, R., Kundzewicz, Z. W., & Benito, G. (2006). Historical hydrology for studying flood risk in Europe. *Hydrological Sciences Journal*, 51(5), 739-764. <http://dx.doi.org/10.1623/hysj.51.5.739>.
- Brisco, B., Short, N., Sanden, J., Landry, R., & Raymond, D. (2009). A semi-automated tool for surface water mapping with RADARSAT-1. *Canadian Journal of Remote Sensing*, 35(4), 336-344. <http://dx.doi.org/10.5589/m09-025>.
- Bui, Q.-T., Nguyen, Q.-H., Nguyen, X. L., Pham, V. D., Nguyen, H. D., & Pham, V.-M. (2020). Verification of novel integrations of swarm intelligence algorithms into deep learning neural network for flood susceptibility mapping. *Journal of Hydrology*, 581, 124379. <http://dx.doi.org/10.1016/j.jhydrol.2019.124379>.
- Calmant, S., & Seyler, F. (2006). Continental surface waters from satellite altimetry. *Comptes Rendus Geoscience*, 338(14-15), 1113-1122. <http://dx.doi.org/10.1016/j.crte.2006.05.012>.
- CBSNews. (2021, July 16). Floods kill more than 125 after record rain fall in western Europe. Retrieved in 2021, July 17, from <https://www.cbsnews.com/news/flooding-in-germany-europe-deaths-record-rainfall-western-europe-2021-07-16/>
- Costanza, R., d'Arge, R., De Groot, R., Farber, S., Grasso, M., Hannon, B., Limburg, K., Naeem, S., O'Neill, R. V., Paruelo, J., Raskin, R. G., Sutton, P., & van den Belt, M. (1997). The value of the world's ecosystem services and natural capital. *Nature*, 387(6630), 253-260. <http://dx.doi.org/10.1038/387253a0>.
- Coulibaly, P., & Dibike, Y. B. (2004). *Downscaling of global climate model outputs for flood frequency analysis in the Saguenay river system. Final Project Report*. Hamilton: Canadian Climate Change Action Fund, Environment Canada. Retrieved in 2021, November 21, from https://www.hydrology.mcmaster.ca/documents/publications_reports/2004_CCAF_Final_Report.pdf
- Döringer, M., & Tockner, K. (2008). Sustainable Riparian Zones: a management guide, In D. Arizpe, A. Mendes & J. E. Rabaça (Eds.), *Morphology and dynamics of riparian zones* (pp. 23-64). Valencia: Generalitat Valenciana.
- European Space Agency – ESA. (2021). *Sentinel Online*. Retrieved in 2021, September 15, from <https://scihub.copernicus.eu/dhus/#/home>
- Federal Emergency Management Agency – FEMA. (2020). *Guidance for flood risk analysis and mapping: floodway analysis and mapping*. Hyattsville: U.S. Department of Homeland Security. Retrieved in 2021, November 21, from https://www.fema.gov/sites/default/files/documents/fema_floodway-analysis-and-mapping.pdf
- Gallopin, G. C. (2006). Linkages between vulnerability, resilience, and adaptive capacity. *Global Environmental Change*, 16(3), 293-303. <http://dx.doi.org/10.1016/j.gloenvcha.2006.02.004>.
- Gartner, J. D., Mersel, M. K., & Lichvar, R. W. (2016). *Hydrologic modeling and flood frequency analysis for ordinary high water mark delineation*. Hanover: U.S. Army Engineer Research and Development Center. Retrieved in 2021, July 17, from <https://erdc-library.erdcren.mil/jspui/bitstream/11681/21573/1/ERDC-CRREL%20TR-16-2.pdf>
- Guedes, S. A. N. R., & Reydon, B. P. (2012). Direitos de propriedade da terra rural no Brasil: uma proposta institucionalista para ampliar a governança fundiária. *Revista de Economia e Sociologia Rural*, 50(3), 525-544. <http://dx.doi.org/10.1590/S0103-20032012000300008>.
- Gupta, J., & van der Zaag, P. (2008). Interbasin water transfers and integrated water resources management: where engineering, science and politics interlock. *Physics and Chemistry of the Earth Parts A/B/C*, 33(1-2), 28-40. <http://dx.doi.org/10.1016/j.pce.2007.04.003>.
- Haddad, E. A., & Teixeira, E. (2015). Economic impacts of natural disasters in megacities: the case of floods in São Paulo, Brazil. *Habitat International*, 45, 106-113. <http://dx.doi.org/10.1016/j.habitatint.2014.06.023>.

- Holway, J. M., & Burby, R. J. (1990). The effects of floodplain development controls on residential land values. *Land Economics*, 66(3), 259-271. <http://dx.doi.org/10.2307/3146728>.
- Instituto Brasileiro de Geografia e Estatística – IBGE. (2006). *Censo agropecuário 2006*. Rio de Janeiro.
- Instituto Nacional de Colonização e Reforma Agrária – INCRA. (2019). *Quilombolas*. Retrieved in 2020, May 20, from <http://www.incra.gov.br/quilombola>
- Instituto Nacional de Colonização e Reforma Agrária – INCRA. (2020). *Assentamentos*. Retrieved in 2020, May 20, from <http://www.incra.gov.br/pt/assentamentos.html>
- Instituto Nacional de Pesquisas Espaciais – INPE. Divisão de Geração de Imagens – DIDGI. (2021). Retrieved in 2021, September 15, from <http://www.dgi.inpe.br/>
- Jain, S. K., Singh, R. D., Jain, M. K., & Lohani, A. K. (2005). Delineation of flood-prone areas using remote sensing technique. *Water Resources Management*, 19(4), 337-347. <http://dx.doi.org/10.1007/s11269-005-3281-5>.
- Janizadeh, S., Avand, M., Jaafari, A., Phong, T. V., Bayat, M., Ahmadisharaf, E., Prakash, I., Pham, B. T., & Lee, S. (2019). Prediction success of machine learning methods for flash flood susceptibility mapping in the Tafresh watershed, Iran. *Sustainability*, 11(19), 5426. <http://dx.doi.org/10.3390/su11195426>.
- Ji, L., Zhang, L., & Wylie, B. (2009). Analysis of dynamic thresholds for the normalized difference water index. *Photogrammetric Engineering and Remote Sensing*, 75(11), 1307-1317. <http://dx.doi.org/10.14358/PERS.75.11.1307>.
- Kang, L., & Jiang, S. (2019). Bivariate frequency analysis of hydrological drought using a nonstationary standardized streamflow index in the Yangtze river. *Journal of Hydrologic Engineering*, 24(2), 05018031. [http://dx.doi.org/10.1061/\(ASCE\)HE.1943-5584.0001749](http://dx.doi.org/10.1061/(ASCE)HE.1943-5584.0001749).
- Kourgialas, N. N., & Karatzas, G. P. (2011). Flood management and a GIS modelling method to assess flood-hazard areas - a case study. *Hydrological Sciences Journal*, 56(2), 212-225. <http://dx.doi.org/10.1080/02626667.2011.555836>.
- Lewis, A. (1998). Geomorphic and hydrologic applications of active microwave remote sensing. In F.M. Henderson & A.J. Lewis (Eds.), *Principles and applications of imaging radar: manual of remote sensing* (pp. 567-629). New York: John Wiley & Sons.
- Lira, J. (2006). Segmentation and morphology of open water bodies from multispectral images. *International Journal of Remote Sensing*, 27(18), 4015-4038. <http://dx.doi.org/10.1080/01431160600702384>.
- Local Government Association. (2021). *Managing flood risk: roles and responsibilities*. Retrieved in 2021, July 15, from <https://www.local.gov.uk/topics/severe-weather/flooding/local-flood-risk-management/managing-flood-risk-roles-and>
- Maillard, P., Gomes, M. F., Pôssa, E., Oliveira, L., Paula, R. A. S., & C6, J. C. V. (2018). The São Francisco flood plain project: determination of the flood plain terrain using water level data and multi-source satellite imagery. In *Proceedings of SPIE Remote Sensing 2018*. Berlin: International Society for Optics and Photonics. <https://doi.org/10.1117/12.2325382>.
- McCoy, R. (2005). *Field methods in remote sensing*. New York: The Guildford Press.
- McFeeters, S. K. (1996). The use of the normalized difference water index (NDWI) in the delineation of open water features. *International Journal of Remote Sensing*, 17(7), 1425-1432. <http://dx.doi.org/10.1080/01431169608948714>.
- Milly, P. C., Betancourt, J., Falkenmark, M., Hirsch, R. M., Kundzewicz, Z. W., Lettenmaier, D. P., & Stouffer, R. J. (2008). Stationarity is dead: whither water management? *Science*, 319(5863), 573-574. PMID:18239110. <http://dx.doi.org/10.1126/science.1151915>.
- Monmonier, M. (1997). *Cartographies of danger: mapping hazards in America*. USA: University of Chicago Press. <http://dx.doi.org/10.7208/chicago/9780226534299.001.0001>.
- National Aeronautics and Space Administration – NASA. (2021). *Earthdata*. Retrieved in 2021, September 15, from <https://earthdata.nasa.gov/>
- Natural Resources Canada. (2018). *Federal flood mapping framework version 2.0*. Retrieved in 2021, July 15, from <https://ui.adsabs.harvard.edu/abs/2016AGUFM.H21A1365E/abstract>
- Nobre, C. A., Marengo, J. A., Seluchi, M. E., Cuartas, L. A., & Alves, L. M. (2016). Some characteristics and impacts of the drought and water crisis in Southeastern Brazil during 2014 and 2015. *Journal of Water Resource and Protection*, 8(2), 252-262. <http://dx.doi.org/10.4236/jwarp.2016.82022>.
- Notti, D., Giordan, D., Cal6, F., Pepe, A., Zucca, F., & Galve, J. (2018). Potential and limitations of open satellite data for flood mapping. *Remote Sensing*, 10(11), 1673. <http://dx.doi.org/10.3390/rs10111673>.
- Paredes-Trejo, F., Barbosa, H. A., Giovannettone, J., Kumar, T. V., Thakur, M. K., Burit6, C. D. O., & Uzcátegui-Briceño, C. (2021). Drought assessment in the São Francisco River Basin using satellite-based and ground-based indices. *Remote Sensing*, 13(19), 3921. <http://dx.doi.org/10.3390/rs13193921>.
- Paulon Girardi, E. (2019). Quest6o agr6ria, conflitos e viol6ncias no campo brasileiro. *Revista NERA*, 22(50), <http://dx.doi.org/10.47946/rnera.v0i50.6611>.
- P6ssa, E. M., & Maillard, P. (2018). Precise delineation of small water bodies from Sentinel-1 data using support vector machine classification. *Canadian Journal of Remote Sensing*, 44(3), 179-190. <http://dx.doi.org/10.1080/07038992.2018.1478723>.

- Pôssa, E., Maillard, P., Gomes, M. F., Silva, I., & Leão, G. (2018). On water surface delineation in rivers using Landsat, Sentinel-1 and Sentinel-2 data. In *Proceedings of SPIE Remote Sensing 2018*. Berlin: International Society for Optics and Photonics. <http://dx.doi.org/10.1117/12.2325725>.
- Roman, P. (2017). The São Francisco interbasin water transfer in Brazil: tribulations of a mega project through constraints and controversy. *Water Alternatives*, 10(2), 395-419. Retrieved in 2021, September 15, from <https://www.water-alternatives.org/index.php/alldoc/articles/vol10/v10issue2/361-a10-2-11/file>
- Roy, E., Rousselle, J., & Lacroix, J. (2003). Flood damage reduction program (FDRP) in Quebec: Case study of the Chaudière River. *Natural Hazards*, 28(2-3), 387-405. <http://dx.doi.org/10.1023/A:1022942427248>.
- Santos, A., Lopes, P. M. O., Silva, M. V., Jardim, A. M. D. R. F., Albuquerque Moura, G. B., Fernandes, G. S. T., Oliveira Silva, D. A., Bezerra da Silva, J. L., Moraes Rodrigues, J. A., Araújo Silva, E., & Oliveira-Júnior, J. F. (2020). Causes and consequences of seasonal changes in the water flow of the São Francisco river in the semiarid of Brazil. *Environmental and Sustainability Indicators*, 8, 100084. <http://dx.doi.org/10.1016/j.indic.2020.100084>.
- Santos, E. S., Jennerjahn, T., Leipe, T., Medeiros, P. R. P., Souza, W. F. L., & Knoppers, B. A. (2013). Origem da matéria orgânica sedimentar no delta estuarino do Rio. *Geochimica Brasiliensis*, 27(1), 37-48. <http://dx.doi.org/10.5327/Z0102-9800201300010004>.
- Sivapalan, M., & Samuel, J. M. (2009). Transcending limitations of stationarity and the return period: process-based approach to flood estimation and risk assessment. *Hydrological Processes: An International Journal*, 23(11), 1671-1675. <http://dx.doi.org/10.1002/hyp.7292>.
- Slater, J. A., Garvey, G., Johnston, C., Haase, J., Heady, B., Kroenung, G., & Little, J. (2006). The SRTM data “finishing” process and products. *Photogrammetric Engineering and Remote Sensing*, 72(3), 237-247. <http://dx.doi.org/10.14358/PERS.72.3.237>.
- Smith, L. C. (1997). Satellite remote sensing of river inundation area, stage, and discharge: a review. *Hydrological Processes*, 11(10), 1427-1439. [http://dx.doi.org/10.1002/\(SICI\)1099-1085\(199708\)11:10<1427::AID-HYP473>3.0.CO;2-S](http://dx.doi.org/10.1002/(SICI)1099-1085(199708)11:10<1427::AID-HYP473>3.0.CO;2-S).
- Tehrany, M. S., Pradhan, B., Mansor, S., & Ahmad, N. (2015). Flood susceptibility assessment using GIS-based support vector machine model with different kernel types. *Catena*, 125, 91-101. <http://dx.doi.org/10.1016/j.catena.2014.10.017>.
- Tiner, R. W. (2016). *Wetland indicators: a guide to wetland formation, identification, delineation, classification, and mapping*. Boca Raton: CRC Press. <http://dx.doi.org/10.1201/9781315374710>.
- Turner, T. L. (2014). The positive impacts of no adverse impact floodplain management. *Water Resources IMPACT*, 16(2), 6-8. Retrieved in 2021, September 15, from <https://www.jstor.org/stable/wateresoimpa.16.2.0006>
- U.S. Department of the Interior – USGS. (2021). *Earth Explorer*. Retrieved in 2021, September 15, from <https://earthexplorer.usgs.gov>
- Wilkinson, J., Reydon, B., & Di Sabbato, A. (2012). Concentration and foreign ownership of land in Brazil in the context of global land grabbing. *Canadian Journal of Development Studies*, 33(4), 417-438. <http://dx.doi.org/10.1080/02255189.2012.746651>.
- Wood, A. P., & van Halsema, G. E. (2008). *Scoping agriculture-wetland interactions: towards a sustainable multiple-response strategy* (Vol. 33). Rome: Food and Agriculture Organization of the United Nations. Retrieved in 2021, September 15, from <http://eprints.hud.ac.uk/id/eprint/18185/1/WoodScopingi0314e.pdf>
- Work, E. A., & Gilmer, D. S. (1976). Utilization of satellite data for inventorying prairie ponds and lakes. *Photogrammetric Engineering and Remote Sensing*, 42(5), 685-694. Retrieved in 2021, September 15, from https://www.asprs.org/wp-content/uploads/pers/1976journal/may/1976_may_685-694.pdf
- Xu, H. (2006). Modification of normalised difference water index (NDWI) to enhance open water features in remotely sensed imagery. *International Journal of Remote Sensing*, 27(14), 3025-3033. <http://dx.doi.org/10.1080/01431160600589179>.

Authors contributions

Philippe Maillard: Conceptualization, Methodology, Formal analysis, Writing - original draft, Translation, Software, Project administration.

Marília Ferreira Gomes: Methodology, Validation, Writing - original draft, Investigation, Data curation.

Évelyn Márcia Pôssa: Methodology, Investigation.

Ramille Soares de Paula: Funding acquisition, Project administration, Validation.

Editor-in-Chief: Adilson Pinheiro

Associated Editor: Fernando Mainardi Fan

APPENDIX A. WATER SURFACE EXTRACTION FROM REMOTE SENSING DATA.

The algorithms of image classification used in this study were chosen based on two previous studies, the results of which were published elsewhere in the two following papers; Pôssa & Maillard (2018) examined the precision obtained with SAR data and Pôssa et al. (2018) concentrated on optical data. The following paragraphs summarise these studies. In both studies the accuracy was measured using a ratio that compares the geometry of the shapes extracted from the images with a reference shape. Equation 1 shows the approach, in which the area of intersection (A_i) between the observed (Cobs) and the reference contours (Cref) of the body of water is divided by the union of both and transformed into a percentage.

$$A_i = \left(\frac{C_{ref} \cap C_{obs}}{C_{ref} \cup C_{obs}} \right) \times 100 \tag{1}$$

SAR data. The precision of SAR data was evaluated in a series of small reservoirs in the city of Belo Horizonte to determine the most appropriate processing chain in order to separate water from land (Pôssa & Maillard, 2018). The study showed that the Support Vector Machine classification algorithm used with only the co-polarised VV band was very robust and yielded high levels of precision (83.8% – 94.7% for three small reservoirs). This research was not directly related to this paper and had a purely theoretical scope to determine the attainable precision for water delineation using Sentinel-1 SAR data.

Optical data. In this second study, a 65 km reach of the São Francisco River was used to test the accuracy of three different satellite sensors: Landsat (OLI), Sentinel-1 (CSAR GRD/IW) and -2 (MSI). For this study, one image of each type was processed and classified in a variety of ways to produce water surface areas that were then compared for accuracy assessment with an interpreted high resolution Planet Scope image. Table A1 shows the main characteristics of these images. All images were acquired within the same four days period in January 2018 with a maximum water stage difference of 10 cm. Five supervised classification algorithms (Random Forest, K-nearest neighbours, Maximum Likelihood Classification, Support Vector Machine and Mahalanobis) and two unsupervised ones (K-means and Expectation Maximisation Cluster Analysis) were tested with all band combinations of each image. On average, Random Forest outperformed all other methods but SVM was slightly better for the SAR data. Following the conclusions of this study, all Sentinel-1 images (36 images) were classified using SVM while the S-2 (32 images) and L-8 (6 images) were classified using K-means. Even though the RF algorithm generated better results, the very good performance of K-means and especially its simplicity and objectivity (no user interference apart from the number of classes) made us choose the latter. Table A2 summarises the best results obtained for the different sensor/band combinations.

Table A1. Some acquisition specifications of the satellite image data used in the water extraction comparison study.

Sensor Imagery	Date	Pixel Size (m)	Stage (cm)	Product level
Sentinel-1 (S-1)	15/01/18	10	223	Level-1 GRD
Sentinel-2 (S-2)	17/01/18	10, 20, 60	217	1C
Landsat/OLI (L8)	18/01/18	30, 60	213	L1TP
PlanetScope	17/01/18	3	217	3A

Table A2. Accuracy by spectral bands and polarizations using the K-means algorithm for the optical data and SVM for the SAR data.

Ranking	Landsat-8		Sentinel-2		Sentinel-1	
	Bands	Accuracy	Bands	Accuracy	Polarization	Accuracy
1	6	86.43	8,12	94.70	VV	93.79
2	3,6	86.22	3,8	94.48	VH	84.97
3	3,7	86.09	8A,11	94.41	VV+VH	82.00
4	6,7	85.92	8,11	94.32		
5	3,6,7	85.88	6,8A,11	94.28		
6	3,4,6	85.73	8,11,12	94.25		
7	7	85.59	11,12	94.24		
8	3,4,6,7	85.53	8A,11,12	94.21		
9	3,4,7	85.46	6,8A,11,12	94.16		
10	4,6,7	85.28	6,11,12	94.13		